Applications of Ni-Al Layered Double Hydroxide as Oxygen Evolution Reaction Catalysts Synthesized by Liquid Phase Deposition Process[†]

OPEN ACCESS

Tatsuya OKAYAMA,[a] Hiro MINAMIMOTO,[a,*,§] and Minoru MIZUHATA[a,b,*,§]

[a] *Department of Chemical Science and Engineering, Graduate School of Engineering, Kobe University, 1-1 Rokkodai-cho, Nada-ku, Kobe 657-8501, Japan*

[b] *Faculty of Chemistry, Jagiellonian University, Gronostajowa 2, 30-387 Kraków, Poland*

* Corresponding authors: minamimoto@godzilla.kobe-u.ac.jp (H. M.), mizuhata@kobe-u.ac.jp (M. M.)

ABSTRACT

The Ni-Al layered double hydroxide materials with high crystallinity were synthesized by the room-temperature liquid process and applied as oxygen evolution reaction (OER) catalysts. It is interesting to note that the OER activity was found to be relatively high in comparison with the Ni-based materials. In addition, the structural analyses and the effects of interlayer anion specie on the OER activity were also evaluated. It was found that the changes in the interlayer anion species from F^- to OH^- resulted in the enhancement of the OER activity. The maintained chemical compositions and crystallinity after the electrochemical measurements were also observed through the X-ray analyses. The present work provides the insights about the possibility of the well-defined structures as the electrodes which were prepared by the unique liquid phase process.

1. Introduction

The alkaline water electrolysis process is recognized as one of the important processes for the sustainable society.[1–4] For the establishment of an effective water electrolysis system, the reduction of the overpotential on the oxygen evolution reaction, which is the anodic reaction, is an urgent problem.[5] The oxygen evolution reaction (OER) is the four-electron and proton transfer process, which leads to the large energy losses in the overall process.[6] It is generally accepted that the platinum group metal oxides, such as IrO_2 or RuO_2, greatly catalyze the OER with long-term stability.[7–9] However, due to the cost and scarcity of rare earths, their large-scale applications are limited even though they exhibit excellent catalytic activity and kinetics. This has been the background for the development of low-cost transition metal materials, especially Ni-based catalysts. To date, various types of alloy materials, such as the Ni-Fe or Ni-Co, have been extensively studied.[10–13] The effects of the coexistence of different metal atoms are responsible for the excellent OER activities, comparable to those of noble metal oxides.[14] In addition, it has been reported that the well-defined layered double hydroxide (LDH) structures can promote the water oxidation with the help of the interlayer anion effects.[15–17] Despite their higher OER activities, high-energy processes such as electroplating, electroless plating, or hydrothermal treatment are required to prepare those materials.[16,18–20] Such high-energy processes often lead to the slight differences in the composition or crystallinity of the materials, which results in the relatively lower reproducibility. Therefore, a much milder preparation process with high reproducibility would be desirable for the preparation of the electrode catalysts.

Various types of metal oxide films can be prepared under ambient conditions using the liquid phase deposition (LPD) method.[21–25] By the LPD method, the high degree of purity and crystallinity with good adhesion and shape-following to the substrate can be achieved. In our previous studies, we reported the successful results on the synthesis of Ni-Al-LDH through the LPD method.[26,27] The LDH structure consists of positively charged octahedral hydroxide layers that are neutralized by interlayer anion species (OH^-, NO_3^-, CO_3^{2-}, or SO_4^{2-}).[28,29] LDH materials have been applied in various fields, such as catalysts, due to their unique structures. The effect of the pH value or the concentration of fluoride ions on the deposited amounts of Ni-Al LDH has been investigated as in our report.[30] The anion exchange property or the interlayer distances of anion exchanged Ni-Al LDHs have also been studied.[29] The anion exchange property of the LDH would have the potential for the modulation of the electrochemical properties. Therefore, the structural analyses that are associated with the electrochemical measurements are expected to be important for the applications of LDH as the electrodes. In the present investigations, we synthesized the Ni-Al LDH materials by the LPD method and applied them as alkaline OER catalysts. We have confirmed their relatively higher OER activities in comparison with those of normal Ni electrodes. In addition, we have also investigated the effects of the interlayer anions on the OER activity and the structural changes in dependence of the electrochemical measurements. The present article would be first insights into the potential applications of unique nanostructured materials as active electrode materials prepared by the mild synthesis method.

2. Experimental

The Ni-Al LDH electrodes were synthesized based on our previous reports.[29,30] For the electrochemical measurements, we deposited Ni-Al LDH on fluorine doped tin oxide (FTO) glass substrates. Firstly, to obtain β-$Ni(OH)_2$, 83 g of $Ni(NO_3)_2 \cdot 6H_2O$ was dissolved in 200 mL ion exchange water, then stirred for 30 min. After that, 28 wt% NH_3 aq. was added to adjust the pH of 7.5. The

---

solution was kept at 50 °C for 3 h to deposit β-Ni(OH)$_2$. The deposited β-Ni(OH)$_2$ was washed with distilled water. To obtain the nickel fluorocomplex solution (mother solution), 2.31 g β-Ni(OH)$_2$ (0.025 mol) and 4.63 mL (5 mol) were dissolved in 250 mL aqueous solution, resulting in the concentration of Ni^{2+} and F$^-$ of 84 mM (mmol dm^{-1}) and 0.5 M (mol dm^{-1}), respectively. For the LPD reactions, 200 mL of distilled water were mixed with the mother solution (35.5 mL) and HF (1.2 mL), then 20 wt% NH$_3$ aq. was subsequentially added to adjust the pH = 8.0. After 2.5 mL of Al(NO$_3$)$_3$·6H$_2$O (0.2 mol L^{-1}) was added for the LPD reactions, the FTO substrates were immersed in the 50 mL solution and kept for 24 h at 50 °C. After the LPD reactions, the as-deposited LDH materials were immersed in 1.0 mol L^{-1} NaOH aq. for 2 h (OH$^-$-LDH-2) and 24 h (OH$^-$-LDH-2) for the anion exchange reactions.

After the drying, the surface structures were analyzed by the scanning electron microscope (SEM; JSM-7100F, JEOL), the energy dispersive X-ray spectroscopy (EDX; JED-2300, JEOL), the X-ray diffraction (XRD; Rigaku Smart Lab) equipped with Cu target and Ge (220) double-crystal monochromator (CuK$_{\alpha}$1: λ = 1.5405 Å (= 154.05 pm)), and the X-ray photoelectron spectroscopy (XPS; JPS-9010, JEOL). Electrochemical measurements were performed using the conventional three-electrode cell. The working, counter, and reference electrodes were Ni-Al LDH supported FTO glass, Pt mesh, and Hg/HgO, respectively. All electrochemical potentials described in this article were referred to the reversible hydrogen electrode (RHE). The electrolyte solution was 1 mol L^{-1} NaOH aq. The electrochemical potential was scanned with the rate of 1 mV/sec using a potentiostat (HZ-7000, Hokuto Denko). The electrochemical surface area was determined by the measurements of double layer capacitance at open circuit potential.[11] The cyclic voltammogram was performed in the range of ±100 mV of open circuit potential with the scan rate (v) of 10, 20, 30, 40, and 50 mV/sec. From CV spectra, the double layer capacitance, C_{DL}, was estimated from the following equation;

$$i_c = v C_{DL}$$

where i_c is the charging current. Then, the electrochemical surface area was obtained by dividing C_{DL} by the specific capacitance (0.040 mF cm^{-2}). All electrochemical data were collected with the solution resistance obtained through impedance measurements at 1.5 V.

3. Results and Discussion

Figure 1 shows the surface of FTO obtained after LPD reactions. It was observed that the whole surface of the FTO was covered with the needle-like structures, which are a characteristic feature of the LDH. According to the previous report, the main reactions for LPD can be given as follows;[26]

$$MF_x^{(x-2n)} + nH_2O \rightleftarrows MO_n + xF^- + 2nH^+$$

$$Al + 6HF \rightleftarrows H_3AlF_6 + \frac{3}{2}H_2$$
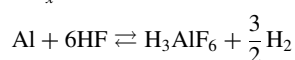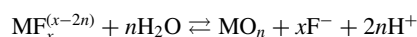
The Al species play as F$^-$ scavenger and lead to the formation of LDH structure. It was reported that the Al amounts have a sensitive effect on the composition of the deposit. Under the present condition, the EDX analyses of the deposits have provided the information about its composition as Ni$_{0.68}$Al$_{0.32}$(OH)$_2$F$_{0.32}$. The interlayer anion of as-deposited Ni-Al LDH (as-dep. LDH) structure was F$^-$. The X-ray diffraction analysis of the deposits was also carried out to evaluate the crystallinity. The peaks at around 10 and 25° correspond to (003) and (006) planes, respectively.[29] The interlayer distance (d_{003}) of 7.8 Å (= 780 pm) was obtained from the peak width of the (003) plane. XRD analysis confirmed the successful synthesis of Ni-Al LDH structures with high crystallinity via room temperature solution process. Incidentally, we did not
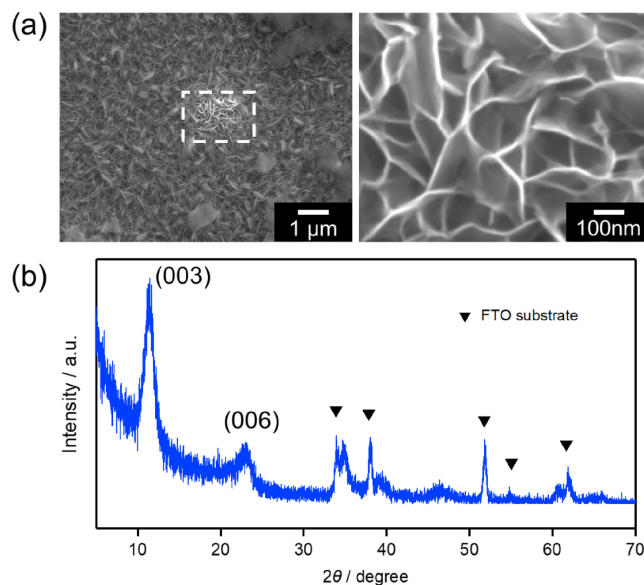

Figure 1. (a) SEM images of as-deposited Ni-Al LDH on the FTO substrate. The right image is the magnified view of the dotted white square in the left image. (b) XRD diffraction pattern of the FTO substrate with the coverage of as-deposited Ni-Al LDH.

perform any decarbonization procedure in the present experiment. Therefore, the possibility of carbonate accommodation cannot be completely excluded.

The cyclic voltammogram (CV) measurements were performed to investigate the OER activities on as-dep. LDH in alkaline solutions as shown in Fig. 2a. All current densities provided in this article were collected using the electrochemical surface area estimated from the electric double layer capacitance as in the experimental section. The electrochemical surface area was almost constant at about 0.16 cm^{-2} for all samples in the present cases. This means that although the deposited amount, which is estimated from the values of the redox current, was slight different on each sample, the surface area for the OER seems to be constant. From this point of view, the collections with the electrochemical surface area would be appropriate. As a comparison, the result of the linear sweep voltammogram on Ni metal plate is also shown in the figure as the black curve. In the case of the Ni metal plate, the surface was reduced at −0.3 V vs. RHE for 3 min to remove the oxidized Ni before the measurement as a pre-treatment. Compared to the normal Ni metal electrode, although the OER activity was slightly decreased after the 3-time scans, it is interesting to note that the as-dep. LDH showed quite higher OER activities. From the CV curve, the value for the Tafel slope was estimated to be 40 mV/dec, which is relatively lower value in comparison with previously reported values on Ni alloy materials. In addition, the current density of 10 mA cm^{-2} was observed at the overpotential of 0.31 V. On the basis of the benchmark reported by McCrory et al., such a lower potential is recognized as the comparable value to that of Ir metal.[11] In addition, the current value for the Tafel sloe of 40 mV/dec is comparable to the previously reported values for various Ni-based alloys or Ni-Fe LDH materials.[31,32] Therefore, the synthesized Ni-Al LDHs have great potential as an anode in the alkaline water electrolysis. Since the LDH structure has the anion species sandwiched with the positively charged metal species, the hypothesis for the origin of the high OER activity on Ni-Al LDH could be considered as the surface anion incorporation, which modulates the chemical and physical properties of the materials. For example, as in the previous reports, fluorine anion doping leads to the enhanced OER activity due to the modulation of adsorption energy of reactive intermediates and
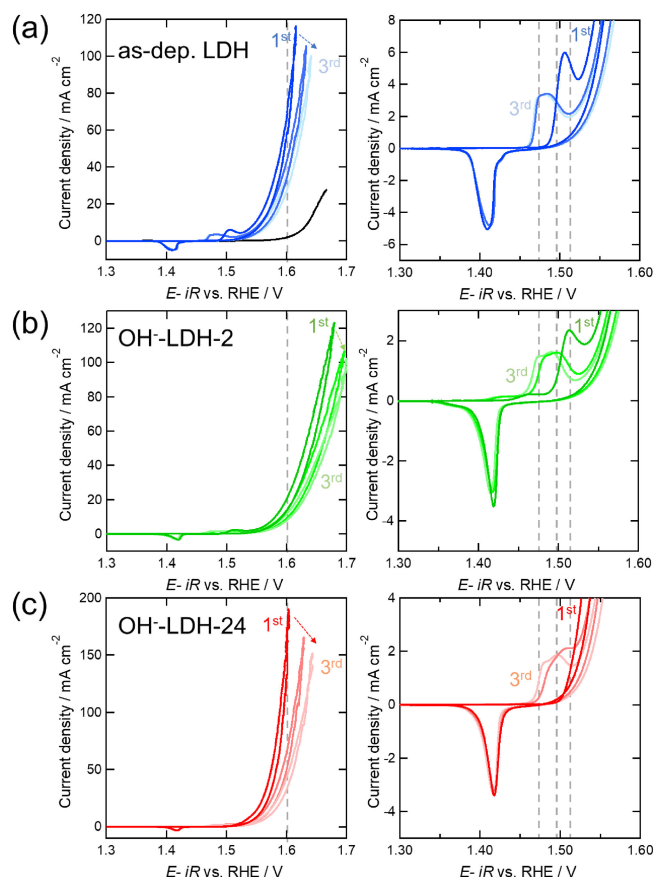
Figure 2. Cyclic voltammogram for (a; blue) the as-dep. LDH, (b; green) OH⁻-LDH-2, and (c; red) OH⁻-LDH-24 obtained in $1\,\mathrm{mol\,L^{-1}}$ NaOH aq. The electrochemical potential was scanned three times as in the figures with the scan rate of 1 mV/sec. The black curve in (a) corresponds to the result for Ni metal plate with the size of $1 \times 1\,\mathrm{cm^2}$. All current densities were collected with the electrochemical surface area.

Figure 3. XRD diffraction patterns of (1) as-dep. LDH, (2, 3) OH⁻-LDH-2, and (4, 5) OH⁻-LDH-24 obtained (1, 3, 5) after and (2, 4) before CV measurements as in Fig. 3. Each interlayer distance of d_{003} was given in the figure.

electronic conductivity.[33,34] Considering this fact, we have further investigated the effects of interlayer anion species on the OER activity.

The anion exchange property of the interlayer is a characteristic feature of the LDH materials. According to our previous report, the interlayer anion can be easily exchanged from F⁻ to OH⁻ ions by simple immersion in NaOH aq. solutions.[29] The pH of the solution influences the anion exchange capacity. Therefore, we obtained Ni-Al LDH with the interlayer anion of OH⁻ (OH⁻-LDH) by immersing FTO electrodes with the coverage of F⁻-LDH in $1\,\mathrm{mol\,L^{-1}}$ NaOH aq. for 24 h (OH⁻-LDH-24). As comparison, the immersion of F⁻-LDH in $1\,\mathrm{mol\,L^{-1}}$ NaOH aq. for 2 h was also performed (OH⁻-LDH-2). The immersion time of 2 h is the same as the time required to obtain the 1st cycle of the cyclic voltammogram (CV) spectrum. The CV for OH⁻-LDH-2 and OH⁻-LDH-24 are shown in Figs. 2b and 2c, respectively. From the CV measurements, it was found that the overpotential at $10\,\mathrm{mA\,cm^{-1}}$ on OH⁻-LDH-24 was decreased (about −0.07 V). It was also confirmed that the OH⁻-LDH-2 has a relatively lower OER activity than even that of as-dep. LDH. From these electrochemical measurements, it was clearly demonstrated that the anion exchange procedure is capable of the modulation of the OER activity on LDH materials. It should be mentioned that the electrochemical surface area was almost constant before and after immersing in the alkaline solution. This means that the dissolution of LDH materials during anion exchange could be negligible.
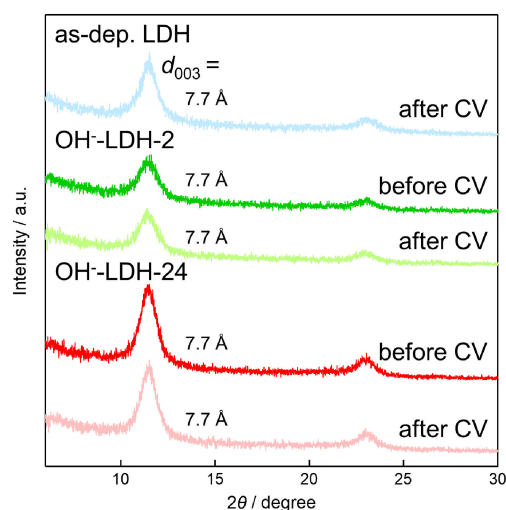
Furthermore, we focused on the anodic peaks observed at about 1.5 V, which reflect the properties to the Ni. The magnified CV spectra were provided in the right panel of Fig. 2. The anodic peak at around 1.5 V on the 1st cycle of as-dep. LDH corresponds to the oxidation of the Ni site from +2 to +3, Ni(OH)₂ to NiOOH.[27] The same peak was also observed on the case for OH⁻-LDH-2. This means that the structural difference between as-dep. LDH and OH⁻-LDH-2 might be small. The peak position was slightly shifted to the positive region. Previous reports showed that the oxidation of Ni species can be suppressed or promoted by the presence of other metal atoms or by the interaction of anionic species.[35,36] Thus, this peak shift originated from the partial anion exchange from F⁻ to OH⁻. In contrast, the distinct anodic curve was not observed on the 1st cycle of OH⁻-LDH-24. This difference in the first cycle is an indication of the results of the anion exchange. From these points, it can be expected that the higher OER activity on OH⁻-LDH-24 would be derived from the enhanced interaction with OH⁻, which led to the formation of the intermediate species and the pass for the OH⁻ within the interlayer structure, while the lower activity on OH⁻-LDH-2 might be caused by the effect of coexisting F⁻ and OH⁻ within the interlayer structures. Although there is the fact that previous report indicated that the OH⁻ anion contribute to the formation of strong interaction with the interlayer water or the consumption of OH⁻ were suppressed by the penetration of OH⁻ from electrolyte, leading to the decrease of local pH changes,[37] at the present stage, there is no experimental evidence to explain the origin for these activity changes.

In addition to above facts, it should be mentioned that the cathodic shifts of the oxidation peak were observed on the 2nd and 3rd cycles in all cases. Interestingly, the peak positions of the anodic peak at 3rd cycle were almost constants for all cases. This behavior would imply that the structure or the changes in the distance between the layers achieved the same after the occurrence of alkaline OER. This point was investigated using XRD measurements for each electrode that were taken before and after the CV measurements, as shown in Fig. 3. See in Fig. 1 for the case of the as-dep. LDH before CV measurement. The XRD spectra indicate that all LDH materials have the high degree of crystallinity even several time electrochemical potential scans. It was important that the d_{003} values of all LDH materials estimated after the CV measurements were found to be constant at 7.7 Å. The d_{003} values
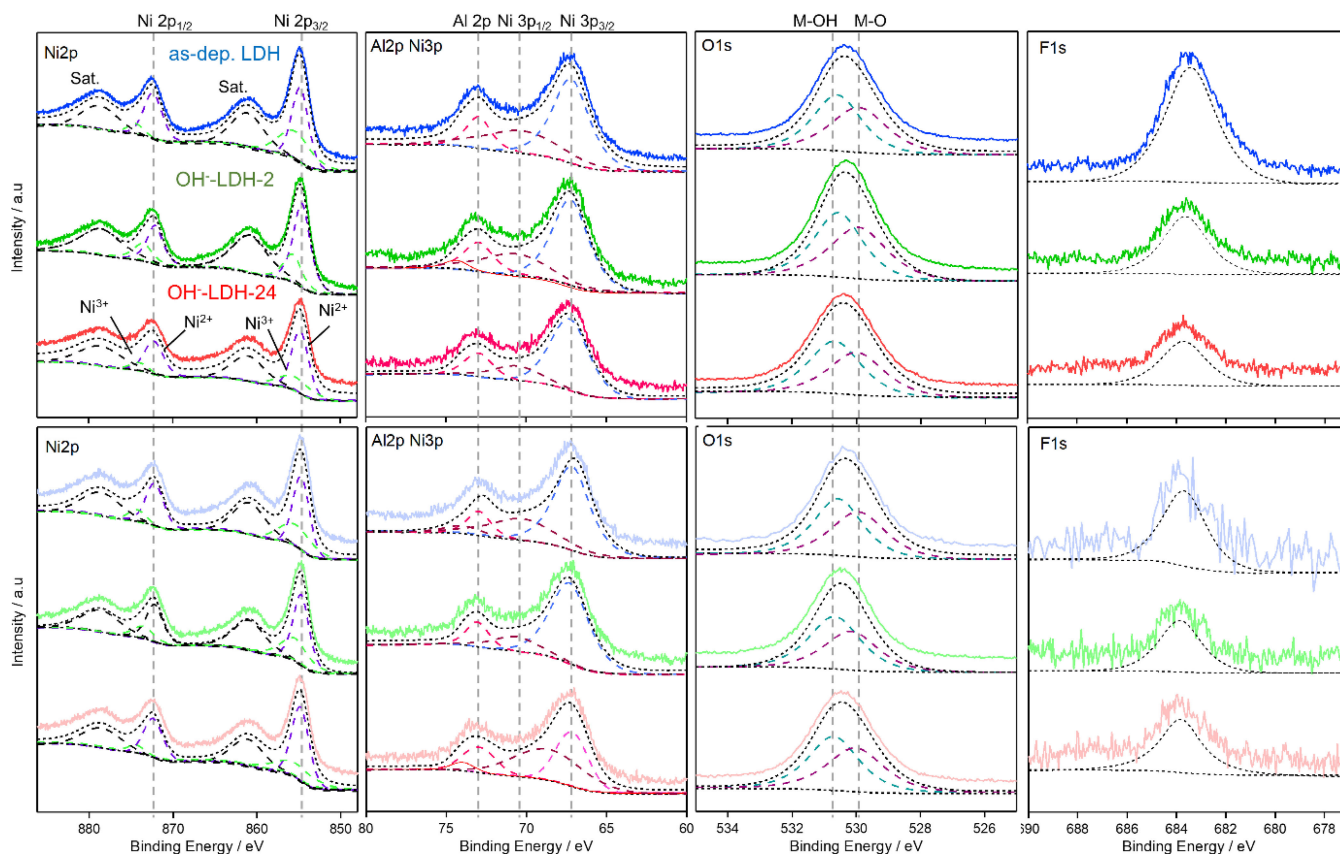
Figure 4. XPS spectra for (blue) as-dep. LDH, (green) OH⁻-LDH-2, and (red) OH⁻-LDH-24, respectively. The upper and bottom panels corresponding to the spectra collected before and after CV measurements, respectively.

for both OH⁻-LDH before CV were also 7.7 Å, indicating that all LDH materials achieved the same structure with the interlayer anion of OH⁻ after the electrochemical measurements. The slight small interlayer distance compared with as-dep. LDH (7.8 Å) would be due to the fact that the ionic radius of OH⁻ (1.37 Å) is smaller than that of F⁻ (1.47 Å). This same structure is good agreement with the electrochemical characteristics as in the CV spectra. Incidentally, that interlayer distance value was slightly thinner than the previously reported value of OH⁻-LDH.[36] The origin of this thinner layer structure could be attributed to the desorption of the interlayer anion during the oxidation of Ni species in the OER process.

Furthermore, XPS analyses were also carried out for the evaluations of materials before and after CV measurements. The XPS spectra collected before and after CV measurements were provided in the upper and bottom panels of Fig. 4, respectively. In all LDH materials, two peaks corresponding to $Ni2p_{1/2}$ and $Ni2p_{3/2}$ which are deconvoluted into Ni^{2+} and Ni^{3+} were observed at 872 and 854 eV, respectively.[38] The peaks at 73, 70, and 67 eV are assigned to the Al2p, $Ni3p_{1/2}$, and $Ni3p_{3/2}$, respectively.[39] It was clear that there was not much difference between the individual materials. The gradual decreases of the peak intensity on F1s from as-dep. LDH to OH⁻-LDH-24 indicate the fact about the changes in the interlayer anion from F⁻ to OH⁻. It was also important that all peak intensities and positions were retained after the OER process in all cases. The fact that there was no incorporation of Fe species or carbonate species in the LDH materials is supported by the absence of changes in the XPS spectra. Therefore, we found that the OER process on LDH results in a reduction of the interlayer distance while maintaining a high degree of crystallinity of the structure. The stable structure after OER processes would have the potential use to evaluate the reaction mechanism of the potential dependent OER

process. On the basis of these structural analyses, the detailed characteristics of the LDH materials prepared by the LPD process under the ambient conditions associated with the electrochemical measurements were revealed.

4. Conclusions

The Ni-Al LDH, which was synthesized by the LPD method, was used as the OER electrode. One of the advantages of the present materials was the relatively high OER activity. In addition to this fact, it was found that the modulation of the OER activity can be achieved by the changes of the interlayer anion species. The stable high crystallinity and the modulations of the interlayer distance during the OER measurements were one of the features of the present material. At present, it is difficult for us to explain the different OER activity depending on the interlayer anion species of F⁻ and OH⁻ which have the similar charge or ionic radius. To reveal this point, not only the appropriate composition of the material, but also the effect of the interlayer species on the OER activity will be investigated as the future work.

Acknowledgments

CRediT Authorship Contribution Statement

Conflict of Interest

Funding

References

1. D. E. Hall, *J. Electrochem. Soc.*, **132**, 41C (1985).
2. C. C. L. McCrory, S. Jung, J. C. Peters, and T. F. Jaramillo, *J. Am. Chem. Soc.*, **135**, 16977 (2013).
3. I. Roger, M. A. Shipman, and M. D. Symes, *Nat. Rev. Chem.*, **1**, 0003 (2017).
4. T. Kou, S. Wang, and Y. Li, *ACS Mater. Lett.*, **3**, 224 (2021).
5. J. S. Kim, B. Kim, H. Kim, and K. Kang, *Adv. Energy Mater.*, **8**, 1702774 (2018).
6. M. Bajdich, M. García-Mota, A. Vojvodic, J. K. Nørskov, and A. T. Bell, *J. Am. Chem. Soc.*, **135**, 13521 (2013).
7. S. Trasatti, *Electrochim. Acta*, **29**, 1503 (1984).
8. T. Reier, M. Oezaslan, and P. Strasser, *ACS Catal.*, **2**, 1765 (2012).
9. Y. Lee, J. Suntivich, K. J. May, E. E. Perry, and Y. Shao-Horn, *J. Phys. Chem. Lett.*, **3**, 399 (2012).
10. J. B. Gerken, S. E. Shaner, R. C. Massé, N. J. Porubsky, and S. S. Stahl, *Energy Environ. Sci.*, **7**, 2376 (2014).
11. C. C. L. McCrory, S. Jung, I. M. Ferrer, S. M. Chatman, J. C. Peters, and T. F. Jaramillo, *J. Am. Chem. Soc.*, **137**, 4347 (2015).
12. L. An, C. Wei, M. Lu, H. Liu, Y. Chen, G. G. Scherer *et al.*, *Adv. Mater.*, **33**, 2006328 (2021).
13. M.-I. Jamesh and M. Harb, *J. Energy Chem.*, **56**, 299 (2021).
14. F. Lu, M. Zhou, Y. Zhou, and X. Zeng, *Small*, **13**, 1701931 (2017).
15. D. Friebel, M. W. Louie, M. Bajdich, K. E. Sanwald, Y. Cai, A. M. Wise *et al.*, *J. Am. Chem. Soc.*, **137**, 1305 (2015).
16. X. Li, X. Hao, A. Abudula, and G. Guan, *J. Mater. Chem. A*, **4**, 11973 (2016).
17. F. Dionigi and P. Strasser, *Adv. Energy Mater.*, **6**, 1600621 (2016).
18. G. S. Thomas, A. V. Radha, P. V. Kamath, and S. Kannan, *J. Phys. Chem. B*, **110**, 12365 (2006).
19. L. J. Yang, X. P. Gao, Q. D. Wu, H. Y. Zhu, and G. L. Pan, *J. Phys. Chem. C*, **111**, 4614 (2007).
20. R. Li, J. Xu, Q. Pan, J. Ba, T. Tang, and W. Luo, *ChemistryOpen*, **8**, 1027 (2019).
21. A. Hishinuma, T. Goda, M. Kitaoka, S. Hayashi, and H. Kawahara, *Appl. Surf. Sci.*, **48–49**, 405 (1991).
22. S. Deki, Y. Aoi, O. Hiroi, and A. Kajinami, *Chem. Lett.*, **25**, 433 (1996).
23. S. Deki, H. Y. Y. Ko, T. Fujita, K. Akamatsu, M. Mizuhata, and A. Kajinami, *Eur. Phys. J. D*, **16**, 325 (2001).
24. S. Deki, S. Iizuka, A. Horie, M. Mizuhata, and A. Kajinami, *Chem. Mater.*, **16**, 1747 (2004).
25. M. Mizuhata, *J. Ceram. Soc. Jpn.*, **130**, 752 (2022).
26. M. Mizuhata, A. Hosokawa, A. B. Béléké, and S. Deki, *Chem. Lett.*, **38**, 972 (2009).
27. A. B. Béléké and M. Mizuhata, *J. Power Sources*, **195**, 7669 (2010).
28. S. Miyata and T. Kumura, *Chem. Lett.*, **2**, 843 (1973).
29. H. Maki, Y. Mori, Y. Okumura, and M. Mizuhata, *Mater. Chem. Phys.*, **141**, 445 (2013).
30. H. Maki, M. Takigawa, and M. Mizuhata, *ACS Appl. Mater. Interfaces*, **7**, 17188 (2015).
31. W. Li, F. Li, H. Yang, X. Wu, P. Zhang, Y. Shan, and L. Sun, *Nat. Commun.*, **10**, 5074 (2019).
32. M. Yu, E. Budiyanto, and H. Tüysüz, *Angew. Chem., Int. Ed.*, **61**, e202103824 (2022).
33. L. Chen, J. Chang, Y. Zhang, Z. Gao, D. Wu, F. Xu, Y. Guo, and K. Jiang, *Chem. Commun.*, **55**, 3406 (2019).
34. Y. Tong, H. Mao, P. Chen, Q. Sun, F. Yan, and F. Xi, *Chem. Commun.*, **56**, 4196 (2020).
35. M. W. Louie and A. T. Bell, *J. Am. Chem. Soc.*, **135**, 12329 (2013).
36. R. R. Rao, S. Corby, A. Bucci, M. García-Tecedor, C. A. Mesa, J. Rossmeisl *et al.*, *J. Am. Chem. Soc.*, **144**, 7622 (2022).
37. D. Zhou, P. Li, X. Lin, A. McKinley, Y. Kuang, W. Liu, W.-F. Lin, X. Sun, and X. Duan, *Chem. Soc. Rev.*, **50**, 8790 (2021).
38. Y. Vlamidis, S. Fiorilli, M. Giorgetti, I. Gualandi, E. Scavetta, and D. Tonelli, *RSC Adv.*, **6**, 110976 (2016).
39. J. G. Baker, J. R. Schneider, J. A. Garrido Torres, J. A. Singh, A. J. M. Mackus, M. Bajdich, and S. F. Bent, *ACS Appl. Energy Mater.*, **2**, 3488 (2019).